Multigrid High-Order Mesh Refinement Techniques for Composite Grid Electrostatics Calculations

THOMAS L. BECK

Department of Chemistry, University of Cincinnati, Cincinnati, Ohio 45221-0172

Received 22 January 1999; accepted 12 August 1999

ABSTRACT: A new method for performing high-order mesh-refinement multigrid computations in real space is presented. The method allows for accurate linear scaling electrostatics calculations over composite domains with local nested fine patches. The Full Approximation Scheme (FAS) multigrid technique is utilized for a sequence of refinement patches of increasing resolution. Conservation forms are generated on coarse scales by additional defect correction terms that counter the local excess fluxes at the boundaries. Formulas are given for arbitrary order, extending the existing technique of Bai and Brandt. Test calculations are presented for a singular source in three dimensions that illustrate the multigrid convergence properties, numerical accuracy, and correct order of the approach. © 1999 John Wiley & Sons, Inc. J Comput Chem 20: 1731–1739, 1999

Keywords: high-order finite differences; multigrid; electrostatics

Introduction

Many computational physics and chemistry problems require consideration of a range of length scales. In protein folding, both short- and long-ranged interactions and competitions between them lead to the final configuration of the molecule.[1, 2] For the interaction between a protein and a nucleic acid or a charged interface, specific ionized groups may contribute significantly to the binding, while distant regions of the molecule have less importance.[3] If one studies the electronic structure of large molecules, there is a concentration of electron density around the atomic nuclei and between atoms in the chemical bonding regions, while often large portions of space exhibit low and smoothly varying density.[4] In numerical simulations of fluid dynamics, specified regions may exist that require a higher resolution treatment locally.[5]

Multiscale methods provide one approach for tackling computational problems exhibiting a range of length scales.[6–9] These methods were developed to overcome convergence problems in iterative solutions of partial differential equations. By utilizing approximations from coarser grids, components of the error on a wide range of length scales can be decimated, typically leading to linear scaling com-

Correspondence to: T. L. Beck; e-mail: becktl@email.uc.edu

Contract/grant sponsor: NSF; contract/grant number: CHE-9632309

CCC 0192-8651 / 99 / 161731-09

puting time with system size. The underlying differential equations can be represented in various ways, including finite differences and finite elements. For the present electrostatics method, high-order finite difference representations are employed.

Based on the physical examples given above and others requiring variable resolution, it is appropriate to develop local mesh refinement strategies in that fine gridding is focused only in those spatial regions that require it.[8] The goal is to maintain the linear scaling property of the multigrid method while minimizing the prefactor in the scaling relation. The computational approach adopted here is to generate a sequence of nested *regular* grids; this strategy allows one to use the existing multigrid routines over the mesh refinement patches with no significant changes. It also allows for the implementation of accurate high-order difference equations on a composite mesh. This approach is to be contrasted with the curved grid generation techniques[10] and adaptive finite elements methods[11] that have been widely applied in scientific and engineering applications.

Bai and Brandt[8] addressed several key issues concerning extension of the FAS multigrid technique to locally refined meshes. First, they developed a full multigrid (λ-FMG) algorithm to restore linear scaling behavior that can be lost when many levels of refinements are used and thus the coarser global grids are themselves visited in a way that scales linearly with the number of levels. The work to accuracy exchange rate λ is the Lagrange multiplier for the grid optimization equations. Second, they determined that the same interpolation order can be used at the mesh boundaries as is used over the rest of the domain. Third, they found that local relaxation sweeps near structural singularities (to be differentiated from source singularities) can restore convergence rates to those observed for problems without singularities. Finally, a second-order conservative differencing method was developed for interior source singularities, when it was found that the only important factor for obtaining accurate solutions far from the singularity was to correctly reproduce the source strength around that singularity. Their local mesh refinement technique was tested on a model two-dimensional problem, the source singularity.

In this article, the Bai and Brandt conservative differencing method is extended to high orders and three dimensions. The method is then successfully tested on a three-dimensional source singularity, the Coulomb potential. First, a review of the FAS multigrid method is given. Next, the high-order conservative FAS differencing forms are derived from general considerations of balancing the fluxes at the boundaries. The three-dimensional conservative forms are obtained by locally averaging the one-dimensional fluxes over surfaces at the boundaries. With the inclusion of the high-order flux corrections, the summation of the defect correction over the mesh refinement is zero to machine precision. The boundary corrections lead to accuracy within the patch which is the same as that for a high-order uniform fine mesh covering the whole domain; with no corrections, serious errors occur over the whole composite domain. Additionally, the accuracy outside the refinement zone is improved over that for the high-order uniform coarse mesh over the whole domain. The correct high-order behavior is thus obtained over the entire composite domain. The only exceptions are the points one grid spacing away from the singularity, where high order is not obtained either on uniform or composite meshes.

Although the source singularity problem may appear to be a simplistic model, the singular nature of the source and resulting long-ranged potential actually provide a severe test for a finite difference solution on a Cartesian grid; Bai and Brandt[8] thus chose this problem (in two dimensions) as a test for their second-order method. In addition, the analytical solution is available so that the magnitude and the order of the errors on the composite domain can be accurately assessed. We have shown in other work on uniform domains that the high-order FAS multigrid method can yield accurate solutions for complicated charge distributions such as atomic electrostatics models, zeolite electrostatics, periodic systems, and many electron atoms and molecules.[12]

High orders are often required to obtain numerically accurate results on three-dimensional grids of reasonable size. Although the methods derived here are general for electrostatics problems, part of our motivation stems from the recent development, along with other groups, of *ab initio* multigrid methods for quantum chemistry.[12–15] In our all electron approach, all particles are represented numerically on the grid, including the nuclear singularities. Previously, we have performed density functional calculations on atoms and small molecules on uniform grids, and it is clear that the majority of the numerical errors originate from the regions around the nuclei. These errors are due both to the finite size of the nucleus on the grid and to the poor numerical representation of the core electron orbitals. The methods developed in this article will be incorporated in our electronic structure codes for both the Poisson and eigenvalue solvers.

Full Approximation Scheme Algorithm

The FAS multigrid technique allows for solution of nonlinear problems, and is well suited for the mesh refinement methods presented below.[6, 8, 9, 16] A two-dimensional schematic of the composite mesh examined here is presented in Figure 1, with two nested patches within a full domain. In the test calculations of the present article, four or five levels were employed, with the coarsest three covering the entire domain (see Fig. 2). The Poisson equation to be solved on the finest patch of the four level problem is written as:

$$L^{h4}U^{h4} = f^{h4}. \tag{1}$$

For this case, L^{h4} is the finite difference Laplacian on the finest scale, U^{h4} is the exact grid solution for the potential on that scale, and f^{h4} is -4π times the charge density for a three-dimensional problem. The current approximation to the exact solution will be written in lower case: for example, the approximate $h4$ solution is u^{h4}. On the next coarser level $h3$, the level $h4$ patch covers only a portion of the level $h3$ domain. The equation to be solved on the $h3$ level is:

$$L^{h3}U^{h3} = I_{h4}^{h3}f^{h4} + \tau^{h3}, \tag{2}$$

where I_{h4}^{h3} is the full restriction operator that performs a weighted local average of the fine scale function, and τ^{h3} is the level $h3$ defect correction given by:

$$\tau^{h3} = L^{h3}I_{h4}^{h3}u^{h4} - I_{h4}^{h3}L^{h4}u^{h4}. \tag{3}$$

The fine-scale function can then be corrected as follows:

$$u^{h4} \leftarrow u^{h4} + I_{h3}^{h4}\left(u^{h3} - I_{h4}^{h3}u^{h4}\right) \tag{4}$$

and further iterations are subsequently performed on the $h4$ level. Here, I_{h3}^{h4} is the interpolation operator. One way to understand the function of the defect correction is to observe that, if the exact solution U^{h4} were passed to level $h3$, no correction would be made. That is, the defect correction causes the level $h3$ equation to "optimally mimic" the level $h4$ problem. Note that τ^{h3} is only defined over the coarse grid points within the interior region of the $h4$ level patch, with zero values outside.

When using multiple scales, the defect correction includes an additional contribution from the previous scale. Here, the example is given of the level $h2$ defect correction computed during the final level $h4$ V-cycle:

$$\tau^{h2} = L^{h2}I_{h3}^{h2}u^{h3} - I_{h3}^{h2}L^{h3}u^{h3} + I_{h3}^{h2}\tau^{h3}. \tag{5}$$

By performing these coarse-grid correction cycles recursively to coarser and coarser scales, errors of all wavelengths can be effectively removed, with only several iterations necessary on the fine scale.

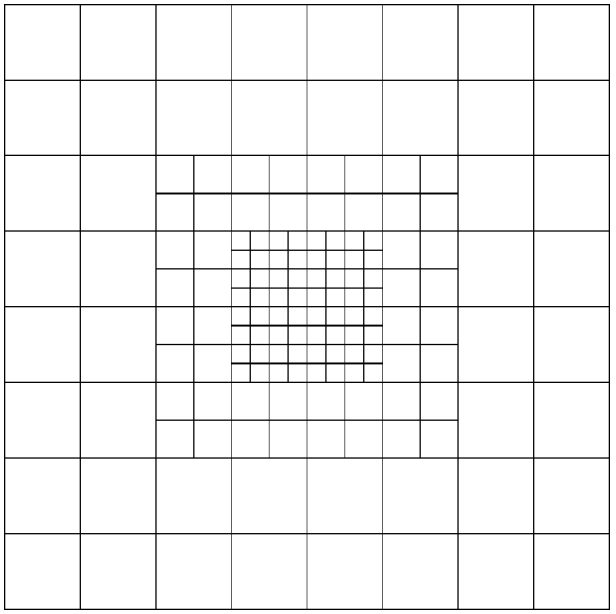

FIGURE 1. Schematic two-dimensional cut through the three-dimensional composite mesh.

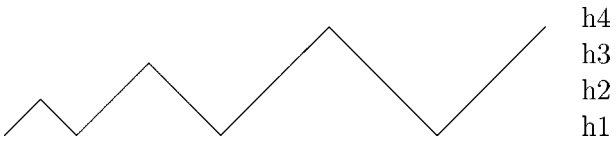

FIGURE 2. Four-level multigrid cycle to solve the FAS equations. The coarsest scale is on the bottom in the diagram. The cycle in the figure starts on the coarsest level and proceeds sequentially to finer scales. Good preconditioning is thus obtained for the initial guess on the finest level. This is referred to as a Full Multigrid (FMG) cycle.

High-Order Conservative Forms

The starting point for developing the required high-order conservative forms is generation of high-order expressions for the Laplacian and interpolation operators. Several methods are available for generating these high-order formulas. Hamming[17] outlines a direct method for obtaining numerical formulas of arbitrary order. This method is quite general because it produces a set of "universal matrices" (one for each order), which, when applied

TABLE I.
Coefficients for the Laplacian.

Points	Order	Prefactor	Coefficients				
$n = 3$	2nd	1				1	−2
$n = 5$	4th	12			−1	16	−30
$n = 7$	6th	180		2	−27	270	−490
$n = 9$	8th	5040	−9	128	−1008	8064	−14350

One side plus the central point are shown. Each coefficient term should be divided by the prefactor. The Laplacian is symmetric about the central point.

TABLE II.
Coefficients for Interpolation.

Points	Order	Prefactor	Coefficients			
$n = 2$	2nd	2				1
$n = 4$	4th	16			−1	9
$n = 6$	6th	256		3	−25	150
$n = 8$	8th	2048	−5	49	−245	1225

One side of the symmetric weight vector is shown. Each coefficient term should be divided by the prefactor.

to a vector of moments for a given operation (differentiation, interpolation, integration), yields the desired coefficients. The matrices are tabulated in ref. 17 up to seven sampling points, which allows for computation up to the sixth order Laplacian. Codes have been written that generate the eight, nine, etc., point matrices as well. The coefficient vectors for the Laplacians through the eighth order are given in Table I. The three-dimensional versions are generated from the sum of the three orthogonal x, y, z axes. We have utilized Laplacians up to twelfth order in previous multigrid work on uniform domains.[12] The interpolation weight vectors for even numbers of sampling points are listed in Table II through eighth order. Similary, formulas for any higher orders can be obtained from the universal matrices.

When solving for the potential on coarser scales that contain a mesh refinement patch at the next finer level, it is clear from eq. (2) that, if the sum of τ over the interior domain is not zero, additional sources have been introduced. This is, in fact, the case, which can be shown by examination of the τ terms in a one-dimensional example; most of the interior terms do cancel, but nonzero contributions remain at the patch boundaries. The terms that remain are of the form of one-dimensional flux operators. Without correcting for these new sources, the solution will be polluted over the whole domain. The method of Bai and Brandt[8] corrects for these sources by introducing local opposing fluxes at the boundary. In this section, their second-order method is extended to high orders.

First, the problem is illustrated schematically by using a continuous notation (in the grid notation, all integrals go over to sums). The coarse scale is labelled by H, and the fine by h. It is desired to satisfy:

$$\int_D \tau^H \, dV = 0, \tag{6}$$

where the integration is over the whole patch domain D, including the boundaries. However, it is true that

$$\int_I \tau_{\text{int}}^H \, dV \neq 0, \tag{7}$$

where τ_{int}^H is the defect correction on the coarse grid points inside the boundaries of the refinement patch, and the integration is only over the interior region I of the patch. Therefore:

$$\int_D \tau^H \, dV = \int_I \tau_{\text{int}}^H \, dV + \int_S \tau_b^H \, dV = 0. \tag{8}$$

Here τ_b^H is a boundary term designed to oppose locally the additional terms due to nonconservation of source and the S integration is over a narrow strip at the surface. This implies:

$$\int_S \tau_b^H \, dV = -\int_I \tau_{\text{int}}^H \, dV. \tag{9}$$

The form of τ_{int}^H is the difference of the Laplacian acting on the coarse scale function minus a local

TABLE III.
Coefficients for Conservative Forms.

Level	Points	Order	Prefactor	Coefficients			
H	$n = 2$	2nd	1				1
h							1
H	$n = 4$	4th	12			−1	15
h						−1	14
H	$n = 6$	6th	180		2	−25	245
h					2	−23	220
H	$n = 8$	8th	5040	−9	119	−889	7175
h				−9	110	−770	6286

One side is shown. Each term on the other half of the gradient operator has the opposite sign. The set of coefficients is for a left boundary. All the signs are reversed for a right boundary. The locations of the terms for a sixth-order example are shown in Figure 3.

average of the Laplacian acting on the fine scale function [eq. (3)]. Therefore, converting a volume integral into a surface integral:

$$\int_S \tau_b^H \, dV = -\int_I \left[(\nabla^2)^H u^H - \left\langle (\nabla^2)^h u^h \right\rangle\right] dV = -\int_\Omega \left[\nabla_b^H u^H - \nabla_b^h u^h\right] d\sigma. \quad (10)$$

The brackets $\langle\,\rangle$ signify a local average (restriction) of the fine scale Laplacian acting on the function, and the gradient operators ∇_b are obtained by noncancellation of terms near the boundary of the volume integral. The final expression shows that the boundary τ_b^H generates a flux that locally opposes the flux from the additional sources in the interior. Therefore, after collecting the correct units from the two scales, it is apparent that the form for τ_b^H is:

$$-\tau_b^H H^2 a = \left[\nabla_b^H u^H - \nabla_b^h u^h\right], \quad (11)$$

where H is the coarse grid spacing, a is the numerical prefactor to the Laplacian (see Table III), and now the gradients are one-dimensional operators directed outward from the surface (determined below). Here the gradients simply represent the unitless coefficients because H^2 and a have been moved to the other side. For example, on a one-dimensional domain (corresponding to the second-order Laplacian):

$$\left[\nabla^H u^H\right]_i = u_i^H - u_{i+1}^H \quad (12)$$

on the left boundary, and

$$\left[\nabla^H u^H\right]_j = u_j^H - u_{j-1}^H \quad (13)$$

on the right.

Because the process of full restriction is a weighted local average over the fine-scale function (27 points in three dimensions), the averaging in eq. (10) can be viewed as follows. First, average over the direction normal to the boundary surface, then compute the two gradient terms on the rhs of eq. (11), and then average over the other two directions. The full restriction weights for this process along one fine-scale dimension are $\mathbf{w} = [1/4\ \ 1/2\ \ 1/4]$. There is no requirement for high-order restriction operators, as long as the same restriction method is used consistently. Therefore, the coefficients for the two gradient terms in eq. (11) can be determined by solving the one-dimensional problem. In two dimensions, the fine-scale gradient operator ∇_b^h is averaged over three points along the boundary line with weights [1/4 1/2 1/4]. This yields a local average of the fine scale flux through the boundary. A similar procedure was followed in the work of Bai and Brandt.[8] In three dimensions, the local flux average is over a square centered on the location of the coarse scale gradient. The weights are 1/4 for the center, 1/8 for the edges, and 1/16 for the corners.

The one-dimensional version of the flux difference in eq. (11) was solved for high orders by examination of the cancellation of terms near the boundary. The result for the left-hand side of the coarse-scale gradient on a left boundary is given by:

$$d_{(-n_L+i)} = \sum_{j=0}^{i} c_{(-n_L+j)}, \qquad i = 0, n_L - 1, \quad (14)$$

where n_L is the number of points in the Laplacian to the left of the center and the $c_{(-n_L+j)}$ are the Laplacian coefficients from Table I. The right side of the gradient is antisymmetric with respect to these coefficients. For a right-side boundary, all the signs are reversed.

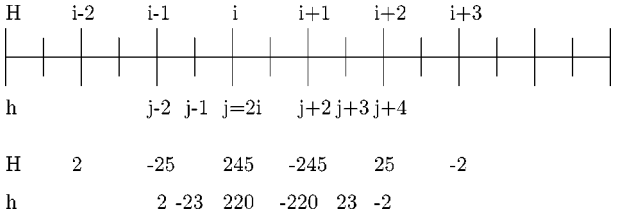

FIGURE 3. Locations and values for the coefficients used to generate the sixth-order conservative form on a left boundary. The boundary is located on the coarse scale *H* at the point *i* and on the fine scale *h* at the point $j = 2i$.

The locally averaged (in one dimension) fine-scale gradient coefficients are:

$$e_{(-n_L+i)} = \sum_{j=0}^{i-1} 2c_{(-n_L+j)} + c_{(-n_L+i)}, \qquad i = 0, n_L - 1. \tag{15}$$

For the fine-scale coefficients, the central term always cancels completely, so both gradient operators ∇_b^H and ∇_b^h are centered about the fine grid location one point inside the patch boundary. All of the coefficients up through eighth order are listed in Table III, and the terms for a sixth order left boundary are shown in Figure 3 to illustrate the locations. Similarly, conservative forms can be derived for higher orders if desired.

Computational Details and Numerical Results

The computational test case presented here is for the fourth-order form. The three coarsest scales covered the whole domain, while the finest one or two were nested patches. On the three coarsest (full domain) scales, the boundaries were set by fixing the potential at the analytical value for a singular source in three dimensions $\phi(\mathbf{r}) = 1/r$. The boundary was fixed with one additional term outside the physical boundary because the Laplacian has two terms beyond the center in one dimension. Iterations were performed over all the interior points of the full domain or patch. The FAS-MG representation was used, and the equations were solved in the form of a series of nested V-cycles, as shown in Figure 2. The progression from coarse scales to fine prior to the V-cycles on the finest level is termed full multigrid (FMG). The purpose is to obtain efficient preconditioning for the initial guess of the fine-scale function. Also, the boundary values for the refinement patches must initially be set using values from the coarse-grid iterations. Because the focus of the present study is the generation of high-order conservative forms, the λ-FMG method in ref. 8 was not implemented here. SOR iterations were employed for all relaxation steps, with $\omega = 1.2$, a near optimal relaxation parameter determined empirically for the high-order case. Simple lexicographic ordering was used for the relaxation sweeps. Full weighting restriction and linear interpolation were used, except fourth-order interpolation was performed over the patch regions, including the required points beyond the boundaries. These points were set such that the Laplacian and defect correction were defined over the entire interior of the patch. The boundary potential terms for the patches were reset during the correction step after each visit to coarser scales.

The code was written in C, with double precision arithmetic, utilizing the prescription of ref. 16 for dynamic memory allocation. The test calculations required a total of roughly 15 relaxation sweeps on the fine scale for convergence in a single fine-scale V-cycle. Convergence as used here means the numerical solution has a value between the exact numerical solution plus or minus the computed error. The "exact" grid results were obtained by repeated loops around the final V-cycle of the FAS procedure, until the residuals were on the order of machine precision zero. The coarsest (full domain) scale had five points on a side, the next two finer scales 9 and 17, and the two nested patches both had 9 points on a side. To examine the order of the method, computations were performed on a full domain coarse grid corresponding to that of the composite mesh (level *h*3), followed by one finer full-domain grid with the spacing halved. The accuracy of the composite mesh method was then determined by comparison with the high-order coarse and fine uniform grid calculations used in the determination of the order.

The increased accuracy obtained using fourth-order equations vs. second order is displayed for uniform domain computations in Figure 4, in which the absolute errors of the solution are presented away from the singularity. That the fourth-order Laplacian leads to fourth-order behavior was confirmed in the uniform grid computations described above. Except for the set of points one grid spacing away from the singularity, the correct order is obtained over the entire domain.

Then computations were performed on the four-level composite domain, with a single refinement patch centered at the origin. To test the effect of the boundary correction on conservation, the integral of the defect correction over the refinement patch

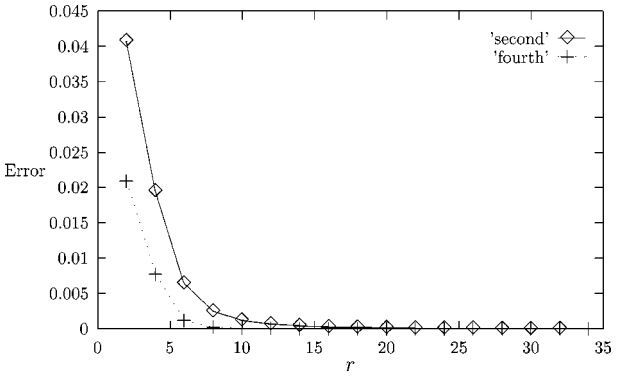

FIGURE 4. Uniform domain calculations illustrating the improved accuracy of the fourth-order approximation over the second-order case. The diamonds are the second-order results, and the crosses are fourth order.

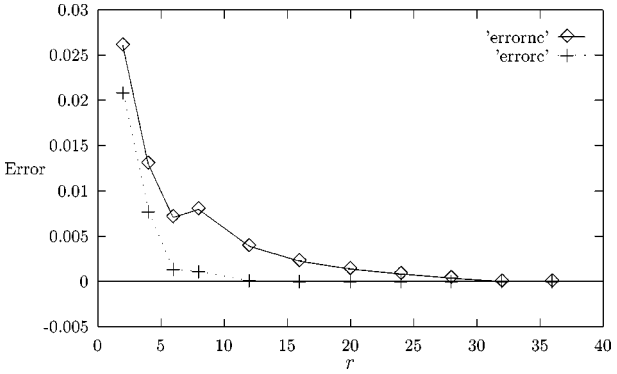

FIGURE 5. Impact of nonconservation on the accuracy. The refinement patch edge is at $r = 8$. The diamonds are for the nonconservative calculation, and the crosses for the conservative case.

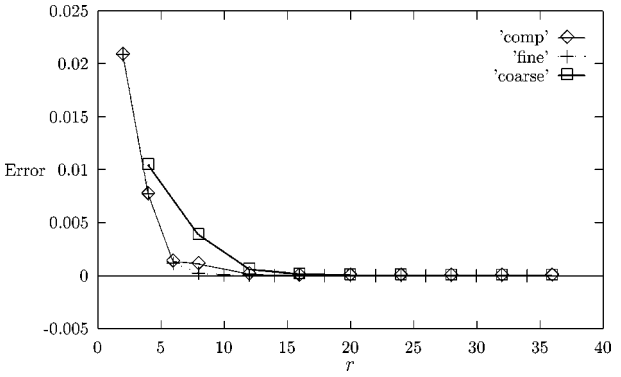

FIGURE 6. Comparison of the accuracy for the composite grid with that on the uniform fine and coarse scales. The refinement patch edge is at $r = 8$. The diamonds are for the composite grid, the crosses for the uniform fine grid, and the squares for the uniform coarse grid. The interior patch points are at $r = 2, 4, 6$.

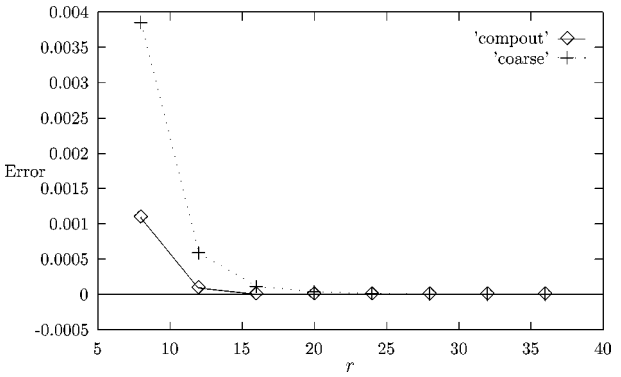

FIGURE 7. Comparison of accuracy outside the refinement patch with the uniform coarse-grid results. The crosses are the uniform coarse grid results, and the diamonds are for the composite grid computation.

was computed with and without the boundary terms. Without the boundary correction, the integral was 0.8 in magnitude, while with the boundary terms, the integral was zero to double precision accuracy. The impact of the conservative boundary correction on the accuracy of the solution is apparent in Figure 5; serious errors are incurred over the whole domain in the absence of the boundary corrections. The accuracy of the method can be determined by comparison with the separate fine and coarse uniform domain results. Figure 6 shows that the accuracy within the patch is virtually identical to that for the uniform fine-domain results. The function value at the $r = 8$ grid point on the composite grid is set by the coarse scale, which results in the larger error there relative to inside the patch. In Figure 7, the errors outside the refinement patch are displayed. The refinement mesh leads to increased accuracy outside the refinement on the coarser level in comparison with the uniform coarse-level results. The numerical results are presented in Table IV. Computations were also performed on a five level problem with two nested refinement patches to test the method on a case with multiple nested refinements. The resulting potential is plotted in Figure 8 to illustrate the accuracy of the method. These numerical results thus confirm that the conservative mesh refinement technique developed here leads to results of the correct high order within the refinement region, while increasing the accuracy on the coarse domain outside the refinement zone.

The above results were generated using fourth-order interpolation over the refinement patch. This was done to match the order of the interpolation (used to set the boundary values for the patch)

TABLE IV.
Numerical Results for the FAS–MG Composite Mesh Computations at Several Distances from the Singular Source.

r	Exact	Grid Exact	Error	Fine Error	Coarse Error	MG Err.
2	0.5	0.520842737	0.020842737	0.020888618		0.020875723
4	0.25	0.257687505	0.007687505	0.007710007	0.010443407	0.007726450
6	$0.1\bar{6}$	0.167993560	0.001326893	0.001183652		0.001389060
8	0.125	0.126091267	0.001091267	0.000232278	0.003854094	0.001232428
12	$0.08\bar{3}$	0.0834252199	0.0000918866	0.0000295553	0.0005908833	0.0001265184
16	0.0625	0.0625022779	0.0000022779	0.0000072359	0.0001151041	0.0000094832
20	0.05	0.0499998476	−0.0000001524	0.0000023526	0.0000347405	0.0000016978
24	$0.041\bar{6}$	0.0416667925	0.0000001258	0.0000008825	0.0000131217	0.0000007387

The edge of the patch is at $r = 8$. The last column is for a single V-cycle MG computation with a total of 16 relaxation sweeps on the fine scale. Notice that for the points in the outer regions of the domain, the single-cycle MG errors are not strictly less than the anomalously small errors for the composite domain; however, the errors are considerably smaller than the errors on the uniform coarse scale domain (they are of the same magnitude as the uniform fine-grid results at those points).

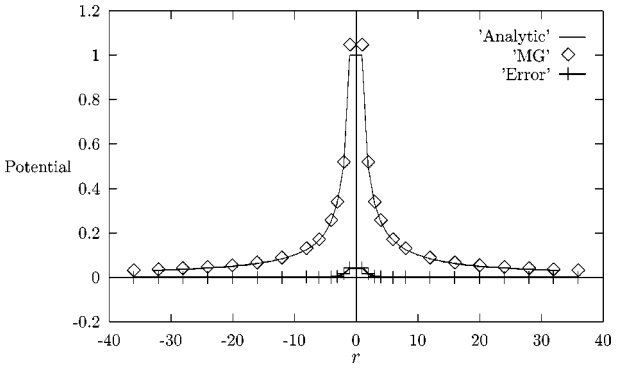

FIGURE 8. Plotted are the analytical $1/r$ potential and the numerical results from the conservative mesh refinement multigrid computation. The two fine patches span the ranges -8 to 8 and -4 to 4. The lower curve (crosses) gives the magnitude of the difference between the exact and numerical results, illustrating the larger errors near the source singularity. The diamonds are MG numerical results on the composite domain, and the line is the analytic result.

with the order of the Laplacian. The results show that the numerical values inside the patch are the same as the fourth-order uniform fine-grid calculation, and indicate that the correct order is obtained over the entire composite domain. Bai and Brandt[8] recommend using an interpolation order of $m + p$, where m is the order of the differential equation, and p is the order of the representation, "to be on the safe side." This would require fifth- or sixth-order interpolation for the present calculation. Our results suggest that order p interpolation is sufficient. To further investigate this issue, a numerical experiment was performed using only linear interpolation for the patch boundaries. Surprisingly, the numerical results also satisfy the accuracy criterion in relation to the uniform domain computations, both inside and outside the patch. However, the errors inside the patch are irregular, and differ from those of the uniform fine-grid calculation, and the errors outside the patch are larger than those using the fourth-order interpolation (but still less than the uniform coarse-grid errors). Therefore, it is suggested that interpolation of the order of the representation is safest, but higher interpolation orders are not necessary. No problems with stability of the high-order interpolation were observed in the calculations.

Summary

A new technique has been presented for carrying out high-order mesh refinement multigrid electrostatics calculations. The FAS method for composite domains was first summarized. Because the sum of the defect correction over the interior of the patch is nonzero, high-order conservative forms were derived by analysis of the one-dimensional problem. The two- and three-dimensional forms can be obtained by averaging locally over three points on a line or nine points on a square, respectively. The new method was successfully tested for the fourth-order case on a Poisson problem, the source singularity in three dimensions.

The high-order mesh refinement methods will allow for accurate electrostatics computations on three-dimensional composite domains. We are developing a quantum chemical Density Functional

Theory (DFT) multigrid method for *ab initio* calculations.[12] So far, our fully numerical three-dimensional calculations have been performed on uniform grids, treating both the electrons and nuclei with the high-order approximations. As a test computation, we examined the CO molecule, and obtained good results in all electron computations. However, it is apparent from those results that the crude treatment of the nuclei and the core electrons limits the accuracy of the method. We plan to incorporate the high-order composite mesh techniques into the quantum chemistry method to obtain more accurate results in the region of the nuclei, and to investigate the impact of those improvements on the eigenfunctions, eigenvalues, and total molecular energies.

Acknowledgments

I thank Achi Brandt, Dov Bai, and Michael Merrick for many helpful discussions. I also thank Daan Frenkel and Bela Mulder for support during a sabbatical leave at the FOM Institute in Amsterdam during the fall of 1996.

References

1. Luthey-Schulten, Z.; Ramirez, B. E.; Wolynes, P. G. J Phys Chem 1995, 99, 2177.
2. Dill, K. A.; Bromberg, S.; Yue, K.; Fiebig, K. M.; Yee, D. P.; Thomas, P. D.; Chan, H. S. Protein Sci 1995, 4, 561.
3. Ben-Tal, N.; Honig, B.; Miller, C.; McLaughlin, S. Biophys J 1997, 73, 1717.
4. Friesner, R. A. Annu Rev Phys Chem 1991, 42, 341.
5. Michelsen, J. A. In Multigrid Methods III; Hackbusch, W.; Trottenberg, U., Eds.; Birkhäuser: Berlin, 1991, p. 301. See other articles in this collection as well.
6. Brandt, A. Math Comp 1977, 31, 333.
7. Briggs, W. L. A Multigrid Tutorial; SIAM: Philadelphia, PA, 1987.
8. Bai, D.; Brandt, A. SIAM J Sci Stat Comput 1987, 8, 109.
9. Brandt, A.; McCormick, S.; Ruge, J. SIAM J Sci Stat Comput 1983, 4, 244.
10. Deconinck, H., Ed. Computational Fluid Dynamics; Von Karman Institute for Fluid Dynamics: Rhode-Saint-Genese, Belgium, 1995; Castillo, J. E., Ed. Mathematical Aspects of Numerical Grid Generation; SIAM: Philadelphia, PA, 1991; Babusa, I., et al., Eds. Modeling, Mesh Generation, and Adaptive Numerical Methods for Partial Differential Equations; Springer Verlag: New York, 1995.
11. Stewart, J. R. S.; Hughes, T. J. R. Finite Elements Anal Design 1997, 25, 1; Jones, M. T.; Plassmann, P. E. ibid 1997, 25, 41; Patra, A.; Oden, J. T. ibid 1997, 25, 27.
12. Merrick, M. P.; Iyer, K. A.; Beck, T. L. J Phys Chem 1995, 99, 12478; Iyer, K. A.; Merrick, M. P.; Beck, T. L. J Chem Phys 1995, 103, 227; Beck, T. L.; Iyer, K. A.; Merrick, M. P. Intl J Quant Chem 1997, 61, 341; Beck, T. L. ibid 1997, 65, 477; Wang, J.; Beck, T. L. 1999, submitted; this paper can also be obtained at xxx.lanl.gov/abs/cond-mat/9905422/; Beck, T. L. In Treatment of Electrostatic Interactions in Computer Simulations of Condensed Media, Hummer, G.; Pratt, L. R., Eds., in press.
13. Gygi, F.; Galli, G. Phys Rev B 1995, 52, R2229.
14. Briggs, E. L.; Sullivan, D. J.; Bernholc, J. Phys Rev B 1995, 52, R5471; ibid 1996, 54, 14362; Bernholc, J.; Briggs, E. L.; Sullivan, D. J.; Brabec, C. J.; Buongiorno Nardelli, M.; Rapcewicz, K.; Roland, C.; Wensell, M. Int J Quant Chem 1997, 65, 531.
15. Fattebert, J.-L. J Comp Phys 1999, 149, 75.
16. Press, W. H.; Teukolsky, S. A.; Vetterling, W. T.; Flannery, B. P. Numerical Recipes in C: The Art of Scientific Computing; Cambridge Univ. Press: Cambridge, 1992.
17. Hamming, R. W. Numerical Methods for Scientists and Engineers; Dover: New York, 1962.